Remote Epitaxy: Fundamentals, Challenges, and Opportunities

Bo-In Park[1,2,†], Jekyung Kim[1,2,†], Kuangye Lu[1,2,†], Xinyuan Zhang[2,3], Sangho Lee[1,2], Jun Min Suh[1,2], Dong-Hwan Kim[4,5], Hyunseok Kim[6,7]*, and Jeehwan Kim[1,2,3,8]**

AUTHOR ADDRESS

[1]Department of Mechanical Engineering, Massachusetts Institute of Technology, Cambridge, MA 02139, USA

[2]Research Laboratory of Electronics, Massachusetts Institute of Technology, Cambridge, MA 02139, USA

[3]Department of Materials Science and Engineering, Massachusetts Institute of Technology, Cambridge, MA 02139, USA

[4]School of Chemical Engineering, Sungkyunkwan University (SKKU), Suwon 16419, Republic of Korea

[5]Biomedical Institute for Convergence at SKKU (BICS), Sungkyunkwan University (SKKU), Suwon 16419, Republic of Korea

[6]Department of Electrical and Computer Engineering, University of Illinois Urbana-Champaign, Urbana, IL 61801, USA

[7]Nick Holonyak, Jr. Micro and Nanotechnology Laboratory, University of Illinois Urbana-Champaign, Urbana, IL 61801, USA

[8]Microsystems Technology Laboratories, Massachusetts Institute of Technology, Cambridge, MA 02139, USA

† These authors contributed equally.

* Correspondence to dhkim1@skku.edu, hyunseok@illinois.edu, jeehwan@mit.edu

KEYWORDS

Remote epitaxy; freestanding membranes; 2D materials; heterogeneous integration

ABSTRACT

Advanced heterogeneous integration technologies are pivotal for next-generation electronics. Single-crystalline materials are one of the key building blocks for heterogeneous integration, although it is challenging to produce and integrate these materials. Remote epitaxy is recently introduced as a solution for growing single-crystalline thin films that can be exfoliated from host wafers and then transferred onto foreign platforms. This technology has quickly gained attention as it can be applied to a wide variety of materials and can realize new functionalities and novel application platforms. Nevertheless, remote epitaxy is a delicate process, and thus successful execution of remote epitaxy is often challenging. Here, we elucidate the mechanisms of remote epitaxy, summarize recent breakthroughs, and discuss the challenges and solutions in remote epitaxy of various material systems. We also provide a vision for the future of remote epitaxy for studying fundamental materials science as well as for functional applications.

Contemporary electronic industries necessitate innovative approaches to incorporate numerous electronic and optoelectronic chips within constrained spaces. This need is particularly pronounced in light of the escalating demand for compact system-on-chip (SoC) designs driven by the popularity of small electronic devices like cellphones, smartwatches, and wearables. Furthermore, the dimensions of fundamental electronic components such as memory, logic circuits, photodetectors, and LEDs have reached their physical constraints in advanced application contexts.[1] Hence, it is crucial to vertically arrange arrays of these devices, making three-dimensional integration one of the foremost priorities in the contemporary electronic community.[2] As is well recognized within this field, these devices must exhibit a single-crystalline structure to achieve optimal electronic and optoelectronic performance. Consequently, layers of such devices are epitaxially grown on the surface of single-crystalline wafers. The process of connecting these single-crystalline devices involves drilling holes through the wafer, known as Through-Silicon Vias (TSV), followed by filling these holes with copper to establish vertical connections.[3] Subsequently, the wafers are bonded together, ultimately creating 3D stacks of devices. Nonetheless, TSV technology encounters practical obstacles, including the expensive wafer grinding process, potential chip misalignment issues, the introduction of RC delay through the copper within the TSV, and the allocation of precious chip space for TSVs.[3] Thus, to enhance the efficiency of the 3D integration process, an ideal approach is the wafer-free stacking of devices, known as monolithic 3D integration.[1,2] One highly effective method for achieving monolithic 3D integration involves creating freestanding single-crystalline membranes and then stacking them.

In 2017, remote epitaxy was introduced to the community as one of the most promising methods for growing single-crystalline electronics and optoelectronics that can be easily separated from the wafer.[4] This method exhibits universal applicability across a wide range of material

systems, facilitates high-throughput membrane manufacturing through exceptionally rapid mechanical release at room temperature, and permits the reuse of substrates, protected by 2D materials.[5] Consequently, it sets itself distinguished from other methods for epitaxial liftoff. The ability of remote epitaxy to generate ultrathin membranes from a wide array of materials also unlocks numerous additional possibilities beyond 3D integration (Fig. 1a). These include applications in flexible electronics and the fusion of functionalities from single-crystalline materials, a feat not typically achievable through conventional heteroepitaxy due to lattice-matching requirements. In this review, we will discuss the applications and opportunities that remote epitaxy brings to the community.

Beyond its promising applications, remote epitaxy represents a novel phenomenon within the epitaxy community, earning its name from the observation that epitaxial films conform to the crystalline lattices of substrates under 2D interlayers. Many research groups worldwide have successfully demonstrated this remote epitaxy phenomenon and expanded the available choice of materials. However, the existence of remote epitaxial phenomena has also been a subject of debate within the community, with several scenarios being considered. Graphene can contain defects, such as dangling bonds, tearing, and residue, which can affect the growth or even lead to a failure of remote epitaxy but could be challenging to observe with advanced microscopy techniques.[6,7] There are other growth mechanisms than remote epitaxy, such as quasi-van der Waals epitaxy and pinhole-based epitaxy, yielding similar results in that single-crystalline thin films are formed on 2D materials.[8,9] As such, this review elucidates the mechanisms of remote epitaxy and the methodologies to unambiguously distinguish the remote epitaxial growth mode from other possible scenarios. For this, several intriguing phenomena are introduced, which are unique to remote epitaxy and theoretically not observable in other growth modes.

It is important to acknowledge that remote epitaxy is a delicate process, typically occurring through one or two layers of graphene, and successful outcomes are highly dependent on specific experimental conditions. Additionally, effective strategies can vary depending on the material systems under investigation. Therefore, this review is intended to provide great details of the methods used to achieve successful remote epitaxy in various material systems.

To conclude, the review will provide a vision of the future of remote epitaxy, with the objective of advancing the electronic industry through revolutionary and exciting applications. In addition to the theoretical and experimental aspects of remote epitaxy, we outline the areas of application enabled by single-crystalline freestanding membranes including advanced electronics, optoelectronics, photonics, and biomedical devices. Furthermore, we summarize the future device platforms and potential discoveries in new physics and phenomena that could emerge from the integration of coupled 3D-3D or 2D-3D mixed heterostructures.

1. Principles of remote epitaxy

In remote epitaxy, single-crystalline thin films are grown on substrates coated with 2D materials, wherein the epilayers are epitaxially aligned with underlying substrates through 2D interlayers (Fig. 1b). Graphene has been dominantly utilized as an interlayer material for remote epitaxy, because graphene does not exhibit polarity and thus has a smaller screening effect than polar 2D materials, such as hexagonal boron nitride (h-BN) and transition metal dichalcogenides (TMDs). When 2D materials do not completely screen the remote interaction between adatoms/nuclei and the substrate, remote epitaxial growth via the 2D interlayer could become possible in principle.[4]

Substrates and 2D materials for remote epitaxy

Since the epitaxial registry in remote epitaxy is governed by the surface potential of the substrate and their attenuation via graphene or other 2D interlayers, the polarity and the orientation of substrate materials critically affect remote epitaxy. A general rule of thumb is that materials with higher ionicity facilitate a stronger interaction of adatoms with substrates via 2D interlayers. For example, III-V compound semiconductors, which exhibit low ionicity, require a very thin, only monolayer, graphene for successful remote epitaxy. On the contrary, ionic materials, such as LiF substrates, can support remote epitaxy up to three layers of graphene, as summarized in Fig. 1c.[10] Above these critical thicknesses of graphene, the substrate potential is almost completely screened by graphene, thereby resulting in the growth dominated by van der Waals interaction between the 2D layer and adatoms. In other words, the critical thickness of graphene for successful remote epitaxy is governed by the ionicity of substrate materials.[10–12]

Such a requirement rules out Si (001) or Ge (001) as a candidate for remote epitaxy, because their covalent-bonded nature makes the surface potential fluctuation too weak for remote epitaxy to occur even with monolayer graphene.[6,10] Nevertheless, the crystallographic orientation of the substrate can also significantly change the intensity of the potential. Based on *ab initio* density functional theory (DFT) calculations, Ge (011) exhibits higher potential fluctuation than Ge (001) as shown in Fig. 1d. This makes a remote epitaxial growth of $BaTiO_{3-\delta}$ (BTO) possible on graphene-coated Ge (011) without any grains, whereas a failure of remote epitaxy of BTO is observed on Ge (001) substrates.[13] This substantiates that not only the substrate materials but also their orientations determine the critical graphene thickness that allows remote epitaxy.

The polarity of 2D materials also plays a significant role in remote epitaxy. Based on DFT calculations, h-BN screens the substrate much more substantially than graphene, resulting in the

coexistence of remote and quasi-van der Waals epitaxy.[5,10] However, this does not mean that 2D materials other than graphene cannot be used in remote epitaxy. In principle, if 2D materials could permit the penetration of the potential field from the substrate, remote epitaxy is still achievable.[5,10,14] The combination of polar 2D materials and substrates with a high ionicity can alleviate the screening effect, as reported by remote epitaxial growth of HfS_2 on monolayer h-BN coated sapphire[14]. Although monolayer TMDs exhibit polarity and are thicker than graphene or h-BN, the utilization of TMDs could also be feasible.

Theoretical studies to unveil remote interaction

Most of the theoretical frameworks on remote epitaxy have been set by DFT calculations. DFT calculations could be applied not only to study the surface properties (such as electric field fluctuation or charge density) of 2D materials-coated substrates, but also to investigate the interactions of adatoms/nuclei with underlying substrates. These studies brought pivotal insights into the role of 2D materials–whether 2D interlayers merely increase the distance between adatoms and the substrate or have any other effects that influence the epitaxy environment.

In initial studies, DFT calculations showed that the potential from the substrate does not completely diminish at the distance set by the thickness of monolayer graphene and van der Waals gap.[4] This suggested the possibility of adatoms to nucleate following the underlying substrate. In the following studies, the transfer of charges from the substrate to the surface of 2D layers is revealed as the fundamental principle of remote epitaxy in given material systems.[10] For example, from DFT calculations of halide perovskite $CsPbBr_3$ (001) on a graphene-coated NaCl(001) substrate,[15] it was found that graphene does not significantly alter the charge distribution at the $CsPbBr_3$ and NaCl interface compared to the case without graphene, thereby leading to remote

epitaxial growth of $CsPbBr_3$ (001) on NaCl (001) (Fig. 2a). Similar phenomena of charge transfer have been also observed in other material systems, such as GaN[16] and GaAs.[5] An atomic relationship of As-C-Ga is thus formed from the remote epitaxy of GaAs, in that the first nucleation layer on graphene is As when the GaAs substrate is terminated with Ga (Fig. 1b).[17]

Theoretical studies with DFT calculations can also quantitatively predict the traits of remote epitaxy. The charge density difference (CDD) calculations showed that charge transfer from the substrate through graphene ultimately enables long-range remote interaction and that the effect could be enhanced with the increasing ionicity of the substrate as shown in Fig. 2b.[18,19] For example, due to improved charge transfer on AlN than Al_2O_3, GaN nucleation density on monolayer graphene-coated AlN should be higher than Al_2O_3, which is experimentally confirmed as well.[18] Recent DFT calculations further modeled that remote epilayers are the most stable when they exhibit the same polarity as the substrate in III-N remote homoepitaxy.[20] For instance, Al-polar AlN substrate will lead to Al-polar AlN while N-polar AlN substrate will result in the formation of N-polar GaN in remote epitaxy. This suggests that adatoms nucleate and eventually follow the same orientation and polarity with the substrate, aided by the charge transfer through graphene in remote epitaxy.

Last, theoretical studies revealed the beneficial roles of graphene. DFT calculations revealed that the potential field is not attenuated within a graphene interlayer but rather propagates across the graphene,[19] which is attributed to the balance by redistribution of π-electrons.[21] Such a relay effect of graphene helps to enlarge the effective distance of the atomic interaction via graphene and thus promotes remote epitaxy further (Fig. 2c). Another beneficial role of graphene stems from its dangling-bond-free nature, which provides a slippery surface for adatoms. Because of this, strain in nuclei can be relaxed spontaneously without introducing dislocations,[12] which is

supported by DFT calculations in that the interface displacement energy on the graphene is much lower than the energy required for introducing dislocations. Thanks to this role of graphene, remote heteroepitaxy systems such as InGaP on graphene/GaAs,[12] GaP on graphene/GaAs,[12] and AlN on graphene/SiC[19] yielded significantly reduced dislocation density compared to direct heteroepitaxy without graphene. These results substantiate that remote heteroepitaxy could be a viable path for improving the crystal quality of epilayers that are lattice-mismatched to the substrate.

Therefore, remote epitaxy offers an attractive path for forming single-crystalline epilayers in diverse material systems. The strain relaxation effect and the capability for mechanical exfoliation make this technology ideal for forming artificial heterostructures by heterogeneous integration.

2. Remote epitaxy: Experimental procedures

As outlined in Fig. 1a, the template for remote epitaxy is prepared by forming 2D materials on substrates. Graphene is the most widely used as an interlayer for remote epitaxy, although remote epitaxy on h-BN has also been reported.[10] To prepare the template, wet transfer of graphene from copper foils to epitaxial substrates has been widely used due to the availability, cost-effectiveness, and thickness-controllability of graphene-on-copper templates.[22] Graphene attained from this process is typically polycrystalline, although single-crystalline graphene can also be produced by using Cu (111) foils.[23] As defects in 2D materials such as grain boundaries and dangling bonds increase the chemical reactivity[24] and induce local fluctuation of surface charge density,[5] the crystallinity of 2D materials could affect the results of remote epitaxy. As another transfer method, dry-transfer processes have been developed for better interface quality. For dry transfer, graphene needs to be first formed on a rigid substrate, exfoliated using a temporary

handling layer, and then directly transferred onto epitaxial substrates.[25] In addition to these transfer methods, transfer-free graphene formation by directly growing graphene on remote epitaxy substrates is recently gaining attention, because direct growth of graphene is more scalable and can eliminate transfer process-related issues. The only obstacle to this approach is that not all substrates are suitable for graphene growth due to the high growth temperature of graphene. Currently, therefore, the reports on remote epitaxy based on directly grown graphene are limited to a few types of substrates, including SiC,[19,26,27] Ge,[13] $SrTiO_3$,[28] and sapphire.[29]

As direct growth of 2D materials is a promising solution for wafer-scale processing with the cleanest interfaces, there have been attempts to directly grow other forms of 2D materials as a remote epitaxy template on the substrates where graphene cannot be grown. For example, GaAs and GaN substrates are thermally unstable at a typical graphene growth temperature, and low-temperature growth processes have been developed to prevent thermally induced damage to these substrates while forming atomically thin carbon layers and boron nitride layers on GaAs and GaN, respectively.[5] These materials are in nanocrystalline or amorphous phases due to their low growth temperatures, but they still dominantly form sp^2-bonds and support remote epitaxy, as shown in Fig. 3a. These low-temperature growth techniques could be utilized for other substrates to expand the available choice of materials for wafer-scale and transfer-residue-free remote epitaxy (Fig. 3b).

Once 2D materials-coated substrates are prepared, remote epitaxy can be conducted on these templates as long as the ionicity of the substrate and the properties of 2D materials are suitable for remote epitaxy.[10] We note that the ionicity of the epitaxial materials is also crucial for successful remote epitaxy, not only that of the substrate, because the interaction between the epilayer and the substrate via graphene is analogous to dipole-dipole interaction.[6] The first experimental demonstration of remote epitaxy was achieved using III-V compound

semiconductors by metal-organic chemical vapor deposition (MOCVD), which is soon followed by many other material systems, including III-N/V,[10] II-VI,[30] I-VII,[10] complex oxides,[11] halide perovskites,[15] and metal[31]. Various epitaxy methods can be utilized for the growth of such a variety of materials, such as gas-based processes including (MO)CVD,[4] molecular beam epitaxy (MBE),[10] evaporation,[31] and pulsed laser deposition (PLD),[11] as well as solution-based processes like hydrothermal methods.[30] The detailed library of material systems and methods for remote epitaxy can be found elsewhere.[32] It is important to note that the epitaxy method can largely affect the results of remote epitaxy, which is discussed in detail in the next section.

As schematically illustrated in Fig. 1a, epitaxial layers and structures formed by remote epitaxy processes can be mechanically exfoliated at the 2D interface due to weak adhesion on 2D materials, which is termed as 2D materials-based layer transfer (2DLT) process. It is even possible to form multiple stacks of remote epitaxial thin films and harvest them layer-by-layer by mechanical peeling,[5] as a high-throughput process for manufacturing freestanding thin films. As 2D materials form a van der Waals (vdW) bonding with both the overlayer and the substrate, it is possible for 2D materials to be exfoliated together with overlayers or remain on the substrate during the 2DLT process.[5,33]

3. Experimental challenges and prospects

Remote epitaxy is a delicate process because it relies on the interaction between substrates and adatoms/nuclei via atomically thin 2D interlayers. Any deviation from ideal atomic configurations could lead to a poor crystal quality of remote epitaxial thin films or even a complete failure of remote epitaxy. The key requirements for successful remote epitaxy are; (a) preparing ideal remote epitaxy templates, (b) preserving the templates during epitaxy, and (c) manipulating

adatoms and nuclei to form thin films with high crystal quality. It is often challenging to achieve them, although satisfying all these requirements is crucial in remote epitaxy. Below we discuss these challenges and solutions in detail.

Preparation of remote epitaxy templates

First, it is critically important to prepare 2D materials-coated substrates exhibiting pristine interfaces and desired 2D material properties. If wet-transferred graphene is employed to form epitaxy templates, it is difficult to keep the graphene/substrate interfaces free of contamination, because liquid trapped at the interface can form residue or induce substrate oxidation during the drying process.[6,8] Interfacial contamination increases the distance between the graphene and the substrate, and thus also the distance between the topmost atoms of the substrate and the bottommost atoms of epilayers, which is confirmed by cross-sectional transmission electron microscopy (TEM) measurements.[17,20] This will severely weaken the remote interaction, and could even lead to the failure of remote epitaxy, as in the example shown in Fig. 3c. Interfacial contamination could also induce a poor epilayer quality,[6] in-plane rotation of nuclei[20] or polycrystalline growth.[17,34] When oxidation of the substrates is severe, 2D materials can even be torn under epitaxy environment due to destructive de-oxidation processes, which can induce nucleation from the damaged 2D area (Fig. 3d).[8,9] These reports substantiate that utilizing wet-transferred graphene is prone to a failure of remote epitaxy and thus should be avoided if possible. Nevertheless, the validity of remote epitaxy has often been studied using wet transfer of graphene.[20,34] Although the interfacial contamination can be mitigated by employing dry transfer processes,[17] graphene inevitably forms wrinkles and tearing regardless of the transfer processes

used, which deteriorates epilayer quality.[4,6] Therefore, it is clear that direct growth of 2D materials is the ideal approach to form pristine interfaces without contamination or substrate oxidation.

For direct growth of 2D materials, CVD-growth of graphene is a viable approach on substrates with good thermal stability.[35] To precisely tune the thickness of graphene layers, atomic layer etching (ALE) of graphene can be used before remote epitaxy to maximize the remote interaction and attain high-quality epilayers.[28] Graphitization of Si-faced SiC substrates is also an effective approach, because the thickness of graphene on SiC can be precisely tuned by sublimation conditions[25] and post-processing[26]. Lastly, amorphous sp^2 materials can potentially be used as a universal remote epitaxy template, because these materials can be grown at low temperatures[36,37] with good controllability of the thickness down to a single atomic layer.[36,38] Indeed, wafer-scale remote epitaxy of III-V and III-N has been achieved using amorphous sp^2 layers as shown in Fig. 3a, proving the effectiveness of such templates.[5]

Preservation of 2D materials during epitaxy

Second, preserving the templates under epitaxy conditions is crucial yet challenging. Epitaxy is usually conducted at high temperatures with reactive agents, and 2D materials can be severely damaged under such an extreme environment. Therefore, the harshness of epitaxy methods/conditions needs to be carefully considered for the successful execution of remote epitaxy. Under MOCVD environment, for example, utilizing hydrogen as a carrier gas could damage the graphene layer, which is experimentally demonstrated in the remote epitaxy of III-V[6] and III-N[39] with graphene interlayers (Fig. 4a). Precursors used for MOCVD growth of these materials, such as trimethylaluminium (TMAl) and ammonia, can also have adverse effects on graphene.[40] These reports on failures of remote epitaxy by damages to 2D materials provide

valuable insights into mitigating the issue. Based on these findings, successful remote epitaxy of III-V and III-N has been achieved by introducing several tactics, such as (a) utilizing nitrogen as a carrier gas,[6,39] (b) introducing low-temperature nucleation stages,[18,29,41] and (c) employing more robust graphene templates, such as graphitized SiC.[19,26] Employing MBE instead of MOCVD could also be an effective approach for the remote epitaxy of these materials,[5,6] because the growth environment is less harsh in MBE as it employs a lower temperature, lower pressure, and elemental sources.

Oxygen is another element that can violently react with 2D materials, which is particularly problematic for the growth of oxides. Even at a very low oxygen partial pressure, graphene is damaged at elevated temperatures.[7] This is observed under both PLD[11] and MBE[7] growths, and is more problematic in growing oxide materials requiring high growth temperatures[11]. Therefore, special tactics have been developed for remote epitaxy of oxides, including (a) starting the growth with thicker graphene to compensate for the partial etching of graphene under epitaxy environment,[11] (b) growing nucleation layers with reduced or no oxygen flow to protect the graphene layer,[11] (c) employing low growth temperatures in MBE, and (d) changing the source materials for oxygen-free growth environment (Fig. 4b).[7]

In addition to the epitaxy environment, there are other factors that affect the stability of graphene during growth. For example, polycrystalline graphene exhibits poorer thermal-chemical stability than single-crystalline graphene, and thus is more easily damaged under epitaxy conditions.[42,43] The stability of substrate materials has to be considered as well, because substrate degradation can entail etching or tearing of graphene. For example, in III-N remote epitaxy by MOCVD, graphene-coated GaN templates are more easily damaged than AlN templates, making remote epitaxy difficult on GaN, as schematically shown in Fig. 4a.[39,41,44] Although not as severe

as GaN, AlN templates can also experience damages under harsh MOCVD growth conditions (Fig. 4c),[18,34,39] while sapphire and SiC templates are the most robust.[19,45] The stability of templates is also affected by the polarity of these substrates (*e.g.* Ga-polar versus N-polar GaN).[46] These results show the importance of experimental designs and the necessity of comprehensive characterizations during/after each process to ensure the pristineness of 2D materials and interfaces for successful remote epitaxy.

Remote epitaxy of high-quality epilayers

Even when the two challenges above are resolved, forming high-quality epilayers by remote epitaxy requires additional careful design of experiments. This is because (a) 2D interlayers screen the electrostatic interaction between adatoms and substrates, and (b) the chemical inertness of graphene surface impedes nucleation of adatoms. First, the chance of forming antisites or defects is increased due to the weakened electrostatic potential by graphene,[10] especially when the substrate exhibits low ionicity. As a result, threading dislocations are formed even when lattice-matched epilayers are grown by remote epitaxy on threading dislocation-free substrates.[5] This suggests that there may be fundamental limitations in forming defect-free epilayers for materials with low ionicity, such as III-V, although more studies are necessary to make a clear conclusion on whether remote homoepitaxy could outperform conventional epitaxy in terms of the material quality. Second, screened electrostatic interaction from the substrate promotes Volmer-Weber growth mode, making it often difficult to form fully merged and planarized thin films.[30] Therefore, the growth conditions need to be modified from standard conditions for enhanced nucleation density.[5,29,47] Intentional formation of dangling bonds on 2D materials by plasma treatment can also be employed in remote epitaxy to enhance the nucleation

density,[29,48] although the conditions used for plasma treatment have to be carefully controlled to prevent the occurrence of other growth modes, such as quasi-vdW (qvdW) epitaxy and pinhole-based selective epitaxy.

Despite such challenges, 2D materials-coated templates also provide unique opportunities for attaining materials with unprecedented properties. First, the dangling-bond-free nature of 2D surfaces offers a path for spontaneous relaxation of strain, meaning that remote heteroepitaxy can be used to produce materials with higher crystal quality than conventional heteroepitaxy.[12,15,19,48] This opens up a new opportunity to grow and exfoliate high-quality membranes that are not lattice-matched to any available wafer. Second, if substrates are defective (*e.g.* typical GaN wafers with high density of threading dislocations), the abrupt junction formed by 2D materials could effectively prevent the crystal defects from extending towards epilayers. This could potentially enable an improvement of epilayer quality in remote homoepitaxy as well, in addition to the case of remote heteroepitaxy, if adequate material systems and growth conditions are employed. Furthermore, graphene can protect the substrate and enable the formation of single-crystal hetero-epilayers that cannot be achieved without graphene, as evidenced by BTO growth on graphene-coated Ge (011).[13] Therefore, remote epitaxy is a versatile technique to study fundamental material science as well as to form high-quality functional membranes.

4. Unveiling the mode of epitaxy

In addition to remote epitaxy, other epitaxy mechanisms are also available on 2D materials-coated substrates. One case is qvdW epitaxy, wherein the nucleation is driven by vdW interaction between adatoms and 2D materials. The substrate underneath 2D materials plays little or no role in the growth. The other case is pinhole-based epitaxy, wherein the nucleation is driven by pinholes

(*i.e*. tiny areas where the substrate is not covered by 2D materials). These pinholes can be formed not only during the transfer of 2D materials[4] but even in directly-grown 2D templates[5] or during the epitaxy on 2D templates (Fig. 3d).[8] Nucleation preferentially occurs in pinholes due to the chemical inertness of 2D materials, and thus, pinhole-based epitaxy can be categorized as a type of selective-area epitaxy with randomly formed patterns. As all these growth modes can yield peelable single-crystalline epilayers, careful studies with rigorous characterizations are necessary to prevent any confusion or misinterpretation of growth results.[49] Furthermore, these growth modes can co-exist if (a) there is non-uniformity in 2D materials, such as thickness fluctuation or damages or (b) more than one growth mode is kinetically allowed. Below we summarize the methodologies to unambiguously distinguish the growth mode.

Remote epitaxy vs. qvdW epitaxy

As the nucleation in remote epitaxy and qvdW epitaxy is governed by underlying substrates and 2D overlayers, respectively, the distinction between these epitaxy modes is straightforward if the in-plane atomic configuration of substrates is not hexagonal (*i.e.* different from 2D materials). In such a case, the mode of epitaxy can be readily verified by comparing the crystal structure of epilayers with that of substrates and 2D materials. Confusion can arise when the substrate has hexagonal in-plane lattices, such as (0001)-oriented wurtzite materials, which coincide with the in-plane lattice configuration of 2D materials. For example, GaN epilayers formed on graphene-coated c-plane sapphire or III-N substrates will exhibit (0001) out-of-plane orientation regardless of the growth mode. Therefore, the in-plane orientation of materials needs to be compared, not the out-of-plane orientation. The growth mode is remote epitaxial if the in-plane orientation of epilayers matches with the substrate, and vice versa. This can be achieved by several measurement

techniques, including in-plane inversion pole figure (IPF) mapping[6,31] and X-ray diffraction (XRD) phi-scan, as shown in Fig. 5a.[10,20] If 2D materials are directly grown on substrates, however, 2D materials and the substrate can also have an epitaxial relationship.[27,48] This makes the verification of the growth mode particularly challenging, because the epilayer, 2D layer, and substrate are all correlated in their in-plane orientation. In this case, studying the thickness dependence can reveal the growth mode. The epilayer quality gets worse or even transforms to polycrystalline phases in remote epitaxy when the thickness of 2D materials is increased,[47,48] whereas the quality is relatively invariant in qvdW epitaxy regardless of the thickness of 2D materials.[50,51] The polarity of 2D materials also plays an important role in substrate screening. This make qvdW epitaxy mode to be favored on h-BN or TMD templates,[10,21,52] although remote epitaxy on these polar 2D materials would not be impossible.

The mode of epitaxy can also be verified by changing the substrate materials while keeping the 2D layer property the same, because changing the substrate will affect the growth results only in remote epitaxy. For example, qvdW epitaxy can yield single-crystalline epilayers on amorphous[53] or polycrystal[20] substrates (Fig. 5b), which is not possible in remote epitaxy. On the other hand, changing the polarity of substrates, such as from N-polar to Al-polar AlN, yields the polarity inversion in epilayers only in the case of remote epitaxy.[20] Lastly, strain relaxation effects are observed in both growth modes, which could be beneficial for growing high-quality ternary materials or lattice-mismatched materials.[54,55] It should be noted, however, that the relaxation is governed only by the 2D materials in qvdW epitaxy mode, whereas the substrate materials (such as the degree of mismatch between the substrate and epilayer) will also affect the relaxation properties in remote epitaxy.[12] These results provide important insights into studying the growth mode.

Remote epitaxy vs. pinhole-based epitaxy

Unlike the case of qvdW epitaxy, the nucleation in pinhole-based epitaxy is governed by underlying substrates, which is the same as remote epitaxy. When pinholes are large and sparse, the epitaxy from pinholes can be easily confirmed by characterizing 2D materials,[8] studying nucleation,[47] and observing the substrate damage during the mechanical exfoliation of epilayers.[4,56] However, if pinholes are (a) small enough (on the order of nanometers) to leave no trace on substrates after epilayer exfoliation and (b) dense enough to provide enough nucleation sites for quick mergence of films, careful studies are needed to distinguish the growth mode.

The most direct method to verify the growth mode is to observe the interface by cross-sectional TEM measurements. In principle, pinhole-based epitaxy can be confirmed by the presence of pinholes and/or direct connection at the epilayer/substrate interface.[27] However, even if no pinhole is observed in TEM images, it does not confirm the remote epitaxial growth because there exists a possibility that pinholes are located 'outside' of the measured area and not detected by TEM. In such a case, the interface may look identical to the case of remote epitaxy. For directly probing remote epitaxy mode in TEM, therefore, it is necessary to stop the growth at a nucleation stage with the nuclei size smaller than a few tens of nanometers, so that TEM specimen can contain the entire nucleus.[47] This completely eliminates the possibility of pinholes residing outside of the lamella made by focused ion beam (FIB) milling, as a direct and irrefutable proof of remote epitaxy (Fig. 5c). In other words, with the lamella containing the entire nucleus can the growth mode be unambiguously verified by adjusting the focus during TEM imaging and confirming the existence (pinhole-based epitaxy) or non-existence (remote epitaxy) of pinholes.

In addition to this direct measurement technique, several indirect methods can be applied to reveal the growth mode. The key idea in these methods is to observe different behaviors of growth in each mode, such as nucleation and strain relaxation characteristics. For example, nucleation density can be used as one of the important indicators to distinguish the growth mode. In pinhole-based epitaxy, the location of pinholes predominantly determines the nucleation sites and also the nucleation density. In remote epitaxy, on the other hand, the diffusion length of adatoms determined by underlying substrates and growth conditions govern the nucleation density. The nucleation density increases in remote epitaxy by (a) changing the substrate material to have larger ionicity[19,47] and (b) decreasing the growth temperature to reduce the diffusion length, as summarized in Fig. 5d.[9,47] In the heteroepitaxy of lattice-mismatched materials, strain properties are also an important indicator in studying the growth mode. Spontaneous relaxation occurs in remote heteroepitaxy, resulting in quick relaxation of entire epilayers at an early stage of growth.[12,13,15,27,48] On the other hand, pinhole-based heteroepitaxy induces strain and defect formation at the exposed area, whereas the laterally overgrown areas are relatively free of strain or defect.[27,56] These features can be characterized by several methods including scanning electron microscopy (SEM), TEM and XRD measurements to reveal the growth mode, as shown in Fig. 5e. Strain in pinhole-based heteroepitaxy can also induce the formation of other domains or facets.[9,27] It is important to note that these two growth modes can co-exist, because completely eliminating pinholes in 2D materials is challenging, if not impossible, although having one growth mode almost completely dominate the other is still possible.[4,6] In this case, verifying the portion of epilayers formed by each growth mode can be informative, which can be systematically studied by tuning the growth conditions (Fig. 5f).[9]

To summarize, distinguishing remote epitaxy from pinhole-based epitaxy may not be trivial after a full growth of merged thin films (especially without growth condition-dependent studies), and a misconception on remote epitaxy could occur if studies are not rigorously designed.[49] To prevent any confusion, it is imperative to study nucleation mechanisms to unambiguously reveal the growth mode by adopting the methods introduced in this section.

5. New functionalities and applications enabled by remote epitaxy

Remote epitaxy provides a chance to monolithically integrate device layers whose crystalline structures are significantly different by permitting the stacking of single-crystalline membranes without any wafer bonding process involved. Moreover, remote epitaxy offers a platform to study mixed-dimensional heterostructures from as-grown 2D/3D heterostructures as well as from detached epilayers that are transferred onto other platforms, forming artificial heterostructures. Below we introduce the new functionalities and applications fields enabled by remote epitaxy.

New paradigm of single-crystalline freestanding membrane production

Several layer transfer techniques have been thoroughly investigated during the last few decades due to their potential in semiconductor device fabrication, serving as a strategy to diminish substrate costs and realize heterogeneously integrated devices. However, the prevalent layer transfer procedures fail to achieve sufficient throughput, cost-efficiency, or enough substrate re-usability to achieve techno-economic benefit. In contrast, 2DLT technique, paired with remote epitaxy, offers multiple advantages over conventional layer transfer methods.

Facilitated by the development of directly grown wafer-scale 2D materials as remote epitaxy templates, 2DLT evolved into a technique that can produce wafer-scale membranes, which was technically challenging in transfer process-based approaches. Furthermore, as the surface of the wafers can be fully covered by direct growth, this enabled high-yield, high-throughput, and low-cost production of freestanding membranes without wafer damages.[5] With direct growth of 2D materials, it even becomes feasible to consecutively grow multiple 3D/2D stacks within a single growth run. A repeated 2DLT process on these stacked wafers can yield multiple membranes with significantly enhanced production throughput, as schematically illustrated in Fig. 6a. Remote epitaxy also brings a substantial cost reduction, because the wafer surface is protected by 2D materials during the exfoliation and thus chemical-mechanical polishing (CMP) processes are not required for wafer recycling. The universality of the process is another huge advantage. Other lift-off techniques like epitaxial lift-off (ELO) and laser lift-off (LLO) require specific substrate properties, whereas remote epitaxy and 2DLT can be applied to a much broader spectrum of materials.[4] This positions 2DLT as a promising method for the heterogeneous integration of diverse membranes.

New functionalities and device applications

Remote epitaxy offers two distinctive features to tackle the issues in industrialization. First, conventional three-dimensional (3D) integration of various optoelectronic and electronic devices relies on drilling holes through the wafer followed by wafer bonding through metals to form interconnects. On the other hand, remote epitaxy enables advanced wafer-free 3D integration, also known as monolithic 3D integration by allowing a 2DLT process, which tackles inherent challenges in conventional wafer-bonding-based 3D integration. Second, conventional

heteroepitaxy suffers from epitaxial strain relaxation by dislocation introduction, which substantially degrades the performance of the devices. However, remote heteroepitaxy enables spontaneous relaxation of strain and reduced dislocation density.[12] Not only the improvement of material qualities, but its impact on enhancing the electrical[57] and optical[15] properties is also demonstrated. Also, as epilayers can be made freestanding by 2DLT process, this provides an additional degree of freedom in manipulating strain-dependent properties of materials.[11,13] This makes remote heteroepitaxy stand out as a unique technique to achieve improved performance in devices that can be made freestanding.

Thus far, there have been various reports on stand-alone optoelectronic devices demonstrated by remote epitaxy. The strain relaxation mechanism in remote heteroepitaxy allowed AlGaN-based deep ultraviolet LEDs (DUV-LEDs) to exhibit enhanced electroluminescence (EL) intensity and quantum efficiency (Fig. 6b).[48,58] Remote epitaxial LEDs that can be made freestanding and are operating in visible wavelengths[4,16] are also demonstrated (Fig. 6c). In addition to emitters, flexible photodetectors with better performance than conventional counterparts are realized by remote heteroepitaxy,[14,59] which also shows the impact of remote epitaxy for making curved/flexible/bendable devices with high performance, as shown in the photograph in Fig. 6d. Vertical stacking of those various devices without having wafer will revolutionize 3D heterogeneous integration. Recently, this has been showcased by demonstrating full-color micro-LED devices by vertically stacking the red, green, and blue LED layers. Owing to its monolithic 3D stacking, the smallest pixel size (4 μm) and the highest array density (5,100 pixels per inch) are demonstrated (Fig. 6e).[60] Similarly, various optoelectronic components could be stacked with driving circuitry made on a Si wafer with 2DLT.

The capability to vertically stack up multiple layers by 2DLT also opens up the path for coupling the physical properties of each layer. For example, a unique multiferroic heterostructure can be formed by stacking piezoelectric lead magnesium niobate–lead titanate (PMN-PT) with remote epitaxial magnetostrictive cobalt ferrite ($CoFe_2O_4$, abbreviated CFO), where both PMN-PT and CFO layers are single-crystalline, allowing for their maximal performance (Fig. 6f).[11] As the substrate clamping effect is eliminated by layer exfoliation and transfer, remarkably high strain-mediated magnetoelectric coupling coefficients are achieved, which were not possible in conventional approaches.

The capability to prepare ultrathin single-crystalline membranes also revolutionizes future bioelectronics because this enables the integration of inorganic single-crystalline semiconductors onto bioelectronic components such as wearables and implantables. For example, declamping from substrates and coupling with functional platforms enabled a new concept of electronic skin (e-skin) devices with multi-modal sensing capabilities.[61] Herein, ultrathin GaN freestanding membranes are produced by remote epitaxy and utilized as surface acoustic wave (SAW) sensors that can measure pulse, sweat, and UV light. The ultrahigh conformability, flexibility, and electromechanical coupling coefficient of freestanding GaN membranes are the key characteristics that lead to efficient wearable devices that can operate wirelessly and without battery (Fig. 6g).

6. Outlook

Although remote epitaxy has a short history of less than a decade, it already emerged as a powerful technique to produce novel single-crystalline membranes. It already proved its usefulness for heterogeneous integration technologies and for studying mixed-dimensional heterostructure, and thus the research community is rapidly expanding worldwide. Nevertheless, the execution of

remote epitaxy is still challenging in many material systems, primarily because of the difficulties in the formation of ideal templates and their preservation during growth. In this review, we summarized the challenges and strategies to overcome these. Eliminating the transfer processes of 2D materials and developing epitaxy strategies specifically targeted for 2D materials templates are the key requirements for successful remote epitaxy. We also explained how remote epitaxial growth mode can be distinguished from other growth modes, with an attempt to address questions on the remote epitaxy mechanisms.

There has been remarkable recent progress in utilizing remote epitaxy for growing materials with unprecedented properties and transferring them to form functional device platforms. Remote epitaxy has a huge potential to be the key technique in monolithic 3D integration of electronics, optoelectronics, photonics, and biomedical devices. Below we introduce prospective future directions that remote epitaxy can uniquely fit into.

In electronics, layer transfer by remote epitaxy can replace current TSV-based interconnects with monolithic integration approaches. High-mobility materials such as III-V can be fabricated into a logic layer and transferred onto a memory layer to construct processing in memory (PIM) architecture. Such a monolithic 3D scheme is regarded as the only viable approach to keep up with Moore's law and achieve a significant boost in data processing speed and efficiency.[1] It is important to note that the transfer of remote epilayers is fully compatible with the back-end-of-line (BEOL) processing constraints, contrary to conventional heteroepitaxy which surpasses the thermal budget required for BEOL compatibility. The key remaining challenges include (a) the need for automation of exfoliation process, (b) the need for adequate bonding process of exfoliated layer, which is compatible with industrial processes, (c) adequate removal and cleaning processes of stressor layers and handling layers, and (d) scaling up the process to be

compatible with industrial wafer sizes. Dedicated research on the engineering aspects of the process is thus necessary for lab-to-fab transition of remote epitaxy technology.

In optoelectronics and photonics, remote epitaxy will allow dissimilar materials and components to be seamlessly integrated on the same plane of a chip. This will be extremely transformative in various applications, including multispectral focal plane arrays (MSFPAs), high-pixel-density and flexible displays for augmented reality/virtual reality (AR/VR), and Si photonic platforms with multi-functionality. Spontaneous relaxation in remote heteroepitaxy will not only enhance the performance but also allow bandgap tunability and expand the wavelengths at which the components/devices/platforms can operate. It should also be noted that these platforms made by remote epitaxy can bypass the cost-intensive and intricate procedures associated with the contemporary wafer-bonding and CMP processes.

In the field of ferroelectrics and multiferroics, remote epitaxy also plays a vital role in producing a variety of freestanding complex-oxide membranes with single-crystallinity, which could serve as an essential building block with unique functionalities for stacking artificial multifunctional heterostructures. The absence of substrate clamping effect in freestanding membranes significantly improves their own functionalities as well as offers an efficient route to control physical properties at the interfaces through active coupling to external perturbations such as strain, light, gating, and proximity. For instance, an unconventional robust ferroelectricity is observed at room temperature in strained STO membrane,[62] and seamless integration of transferrable ultrahigh-κ STO layer onto 2D semiconductor allows for surpassing the performance limits of current 2D transistors.[63] In addition, as discussed in the above section, when material components are all freestanding and single-crystalline, a strain-mediated magnetoelectric coupling effect can be maximized at the interfaces between piezoelectric BTO and magnetostrictive CFO,

where both layers can be generated by remote epitaxy. Such integrated multiferroic material systems with highest efficiency are expected to push the frontier of energy harvesting devices and next-generation logic transistors beyond traditional energy conversion limitations. The flexible, conformal, and wirelessly operating nature of ultrathin multifunctional devices herein holds great promise for future applications such as Internet of Things, smart vehicles, wearable electronics, and biomedical devices.

In conclusion, remote epitaxy technology provides unique opportunities for producing diverse types of single-crystalline membranes, where these membranes will serve as an important building block for next-generation hetero-integrated device platforms.

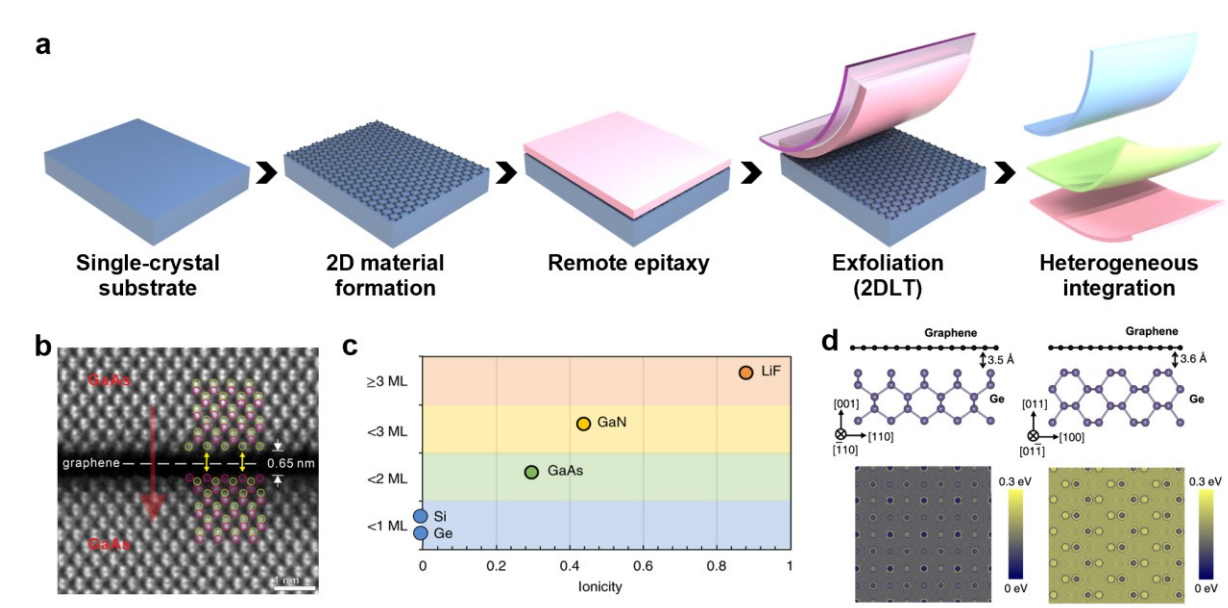

Figure 1. Processes and principles of remote epitaxy. a, Process flow of remote epitaxy and heterogeneous integration. **b,** Cross-sectional STEM image of GaAs on a graphene-coated GaAs, showing atomic alignment via graphene.[17] Adapted with permission from ref 17. Copyright 2021 AIP Publishing. **c,** The maximum graphene thickness allowing for remote interaction as a function of the ionicity of materials.[10] Adapted with permission from ref 10. Copyright 2018 Springer Nature. **d,** DFT calculations showing a stronger surface potential fluctuation on graphene/Ge(011) than graphene/Ge(001).[13] Adapted with permission under the Creative Commons CC BY license from ref 13. Copyright 2022 Springer Nature.

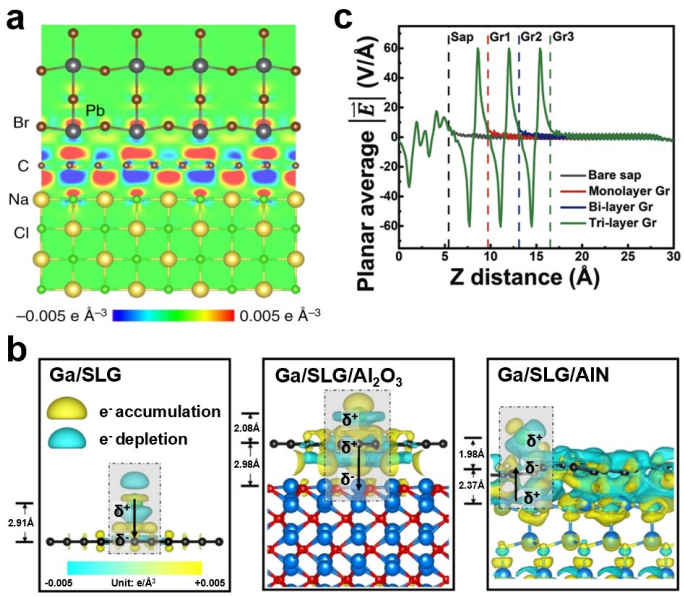

Figure 2. Mechanisms of remote interaction through graphene. a, Charge transfer distributions between $CsPbBr_3(001)$ and NaCl(001) with a graphene interlayer.[15] Adapted with permission under the Creative Commons CC BY license from ref 15. Copyright 2019 Springer Nature. **b,** Charge distribution densities of Ga/single-layer-graphene (SLG), Ga/SLG/Al_2O_3, and Ga/SLG/AlN. Charge redistribution is observed by introducing substrates, and more charge transfer is observed on AlN than Al_2O_3.[18] Adapted with permission from ref 18. Copyright 2022 American Chemical Society. **c,** Calculated planar average electric field of sapphire with various graphene thicknesses, revealing a relay effect.[21] Adapted with permission from ref 21. Copyright 2023 John Wiley and Sons.

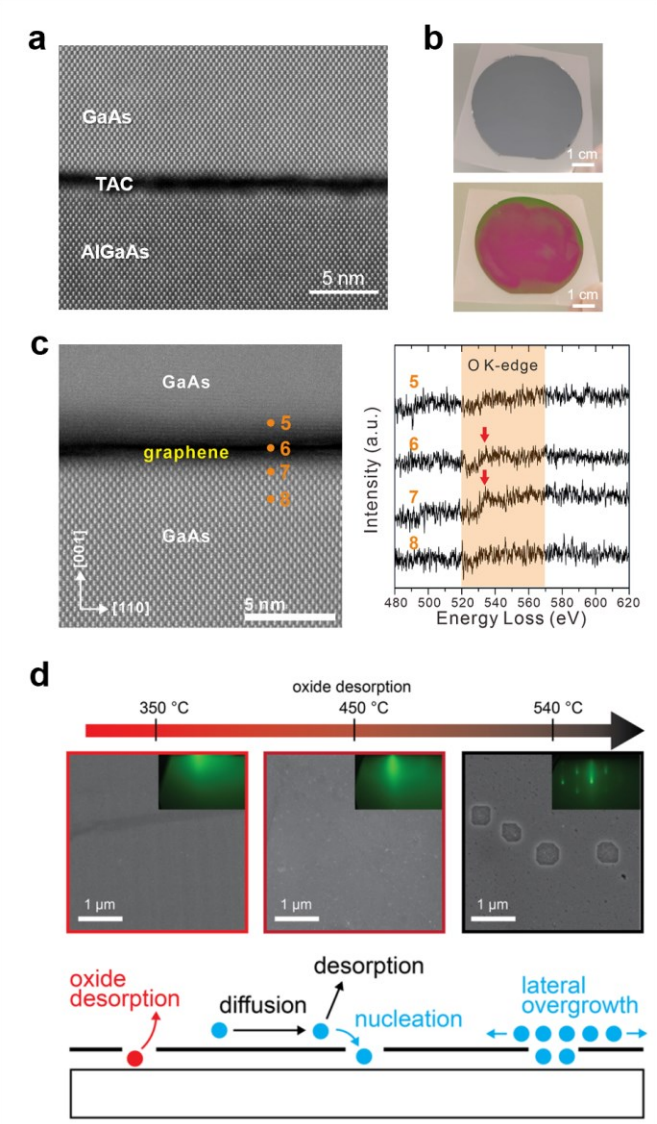

Figure 3. The impact of 2D materials formation methods on remote epitaxy. **a,** Cross-sectional STEM of remote epitaxial GaAs on a directly grown thin amorphous carbon (TAC) layer.[5] Adapted with permission from ref 5. Copyright 2023 Springer Nature. **b,** Photographs of GaAs (upper) and GaN (lower) membranes obtained by remote epitaxy on directly grown 2D materials.[5] Adapted with permission from ref 5. Copyright 2023 Springer Nature. **c,** Cross-sectional STEM of GaAs grown on wet-transferred graphene, showing a failure of remote epitaxy (left). Electron energy loss spectroscopy (EELS) confirms oxidation of graphene/substrate interface.[17] Reprinted from ref 17, with the permission of AIP Publishing. **d,** SEM images and

Reflection high-energy electron diffraction (RHEED) patterns showing a desorption of native oxide and a creation of holes (upper). Schematic (lower) shows the mechanism of pinhole-based selective area epitaxy.[8] Adapted with permission under the Creative Commons CC BY license from ref 8. Copyright 2022 Springer Nature.

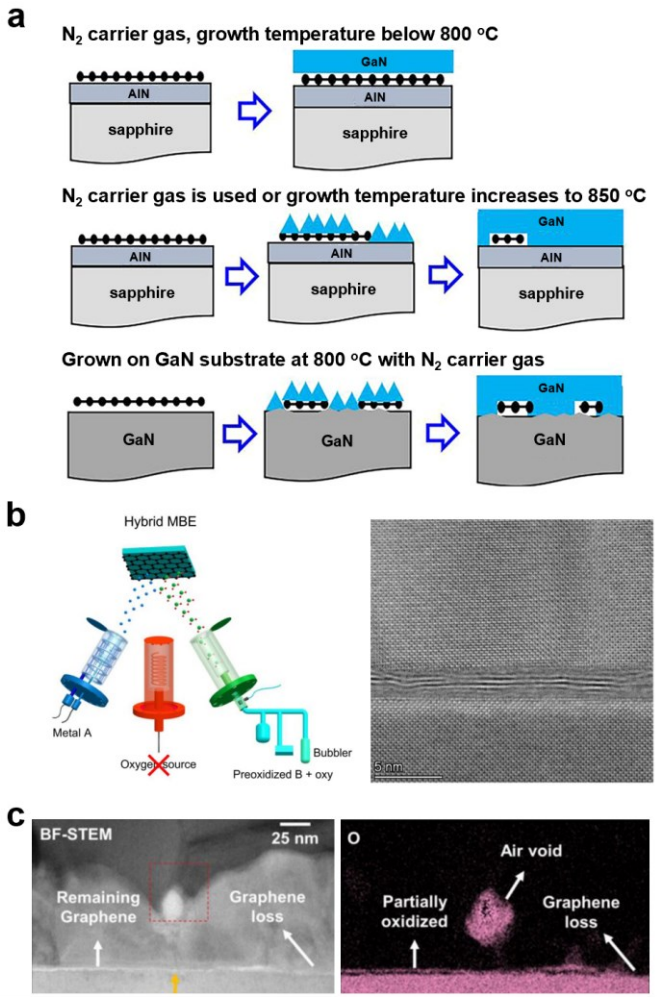

Figure 4. Preservation of 2D materials under epitaxy environment. a, Schematic showing the damage to graphene layer under epitaxy environment, which is more severe under hydrogen environment than nitrogen, and on GaN substrates than AlN.[39] Adapted with permission from ref 39. Copyright 2022 American Chemical Society. **b,** Oxygen-free hybrid MBE to avoid graphene damage (left). Cross-sectional STEM reveals successful remote epitaxy of STO on graphene/STO.[7] Reprinted with permission of AAAS from ref 7. © The Authors, some rights reserved; exclusive licensee AAAS. Distributed under a CC BY-NC 4.0 license (https://creativecommons.org/licenses/by-nc/4.0/). **c,** Failure of III-N remote epitaxy due to graphene damage and interfacial contamination, confirmed by STEM (left) and EDS (right). This

shows the importance of graphene formation method and epitaxy conditions for successful remote epitaxy.[34] Adapted with permission from ref 34. Copyright 2023 AIP Publishing.

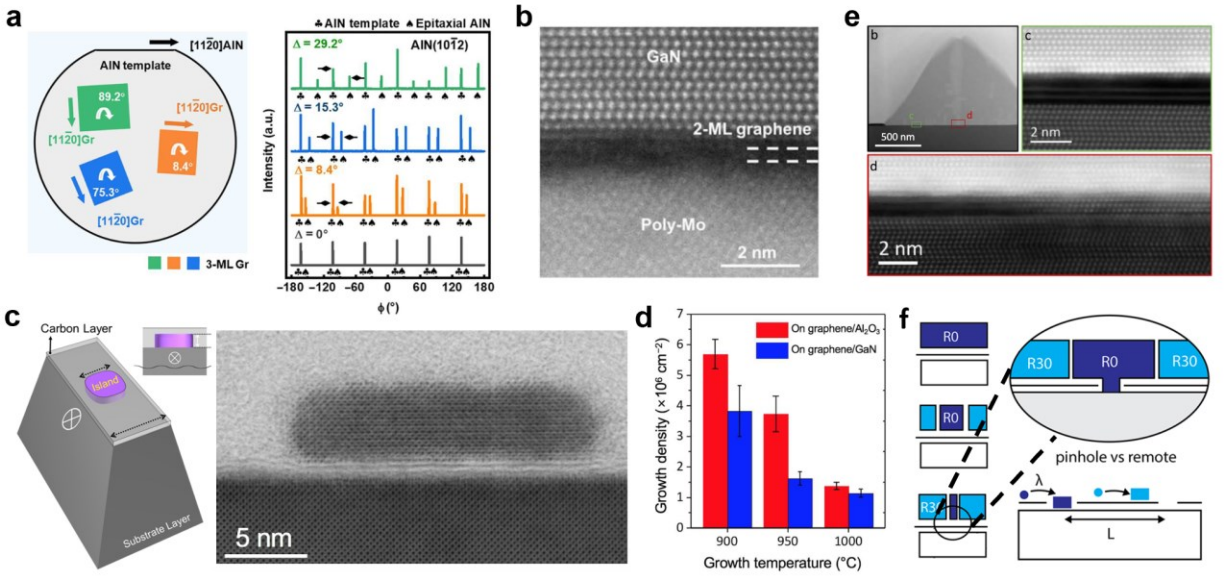

Figure 5. Comparison of qvdW epitaxy, remote epitaxy, and pinhole-based epitaxy. a, In qvdW epitaxy of AlN, the orientation of AlN follows that of graphene, as confirmed by XRD phi-scan.[20] **b,** Cross-sectional STEM image showing single-crystal GaN growth on a polycrystal substrate by qvdW epitaxy.[20] (a,b) Reprinted with permission of AAAS from ref 20. © The Authors, some rights reserved; exclusive licensee AAAS. Distributed under a CC BY-NC 4.0 license (https://creativecommons.org/licenses/by-nc/4.0/). **c,** Confirming the remote epitaxial growth of BTO on graphene/STO by making a TEM specimen containing the entire nuclei (left) and then confirming a full coverage of graphene by STEM (right).[47] **d,** The effect of growth temperatures and substrate ionicity on the nucleation density in remote epitaxy of GaN.[47] (c,d) Reprinted with permission of AAAS from ref 47. © The Authors, some rights reserved; exclusive licensee AAAS. Distributed under a CC BY-NC 4.0 license (https://creativecommons.org/licenses/by-nc/4.0/). **e,** Cross-sectional STEM images of GaN nuclei on epitaxial graphene/SiC. Strain-induced color contrast is observed near the center of the nucleus (upper left). Direct bonding of GaN/SiC is shown in the pinhole area (box 'c'), whereas graphene is fully covered in laterally overgrown area (box 'd').[27] Adapted with permission from ref 27.

Copyright 2019 IOP Publishing, Ltd. **f,** Schematic illustration showing co-existence of remote epitaxy (R30) and pinhole-based epitaxy (R0) areas with different in-plane orientation.[9] Adapted with permission from ref 9. Copyright 2022 American Chemical Society.

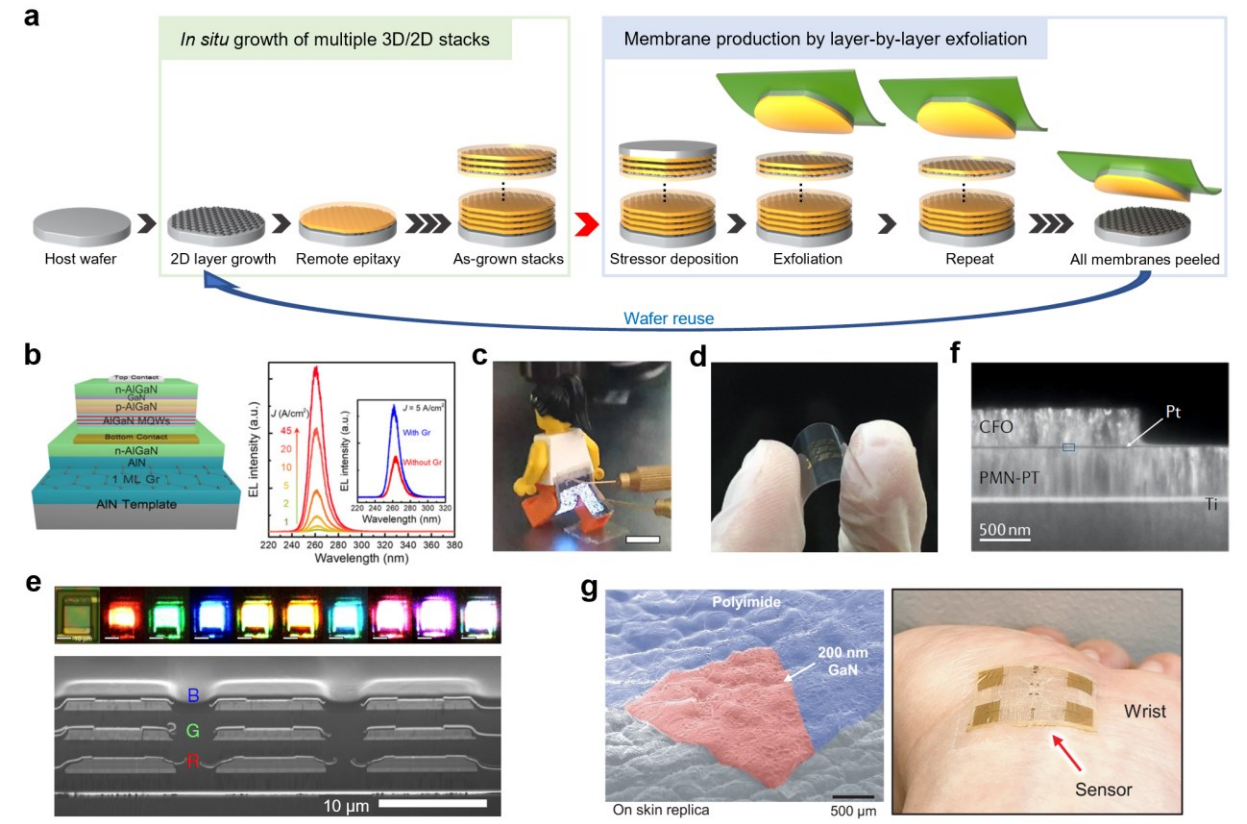

Figure 6. New functionalities and applications by remote epitaxy. a, High-throughput membrane production scheme by multi-stacked remote epitaxy structures.[5] Adapted with permission from ref 5. Copyright 2023 Springer Nature. **b,** Improvement of electroluminescence efficiency of UV LEDs by remote heteroepitaxy.[58] Adapted with permission from ref 58. Copyright 2020 AIP Publishing. **c,d,** Photographs of flexible LEDs[16] (**c**) and photodetectors[14] (**d**) enabled by remote epitaxy. Reprinted with permission of AAAS from ref 16. © The Authors, some rights reserved; exclusive licensee AAAS. Distributed under a CC BY-NC 4.0 license (https://creativecommons.org/licenses/by-nc/4.0/). Adapted with permission from ref 14. Copyright 2019 Royal Society of Chemistry. **e,** Cross-sectional SEM image of vertically stacked RGB micro-LEDs (lower) and photographs showing full-color operation (upper).[60] Adapted with permission from ref 60. Copyright 2023 Springer Nature. **f,** Cross-sectional TEM image of

multiferroic CFO/PMN-PT heterostructure.[11] Adapted with permission from ref 11. Copyright 2020 Springer Nature. **g,** Tilted SEM image (left) and photograph (right) of remote epitaxial GaN membranes on e-skin platforms.[61] Adapted with permission from ref 61. Copyright 2022 American Association for the Advancement of Science.

AUTHOR INFORMATION

Corresponding Author

*Dong-Hwan Kim (dhkim1@skku.edu), Hyunseok Kim (hyunseok@illinois.edu), and Jeehwan Kim(jeehwan@mit.edu)

Author Contributions

†B.-I.P., J.K., and K.L. contributed equally.

Notes

The authors declare no competing financial interest.

ACKNOWLEDGMENT

This work is supported by the Defense Advanced Research Projects Agency Young Faculty Award (award no. D19AP00037-07), the U.S. Department of Energy's Office of Energy Efficiency and Renewable Energy (EERE) under the Solar Energy Technologies Office (award no. DE-EE0008558), Air Force Office of the Scientific Research (AFOSR) (award no. FA9550-22-1-0024), and National Science Foundation (award no. DMR-2240994 and ECCS-2328839). Hyunseok Kim acknowledges support from Samsung GRO program. Jekyung Kim, Bo-In Park, and Dong-Hwan Kim acknowledge support by Korea Institute for Advancement of Technology (KIAT) grant funded by the Korea Government (MOTIE) (P0017305, Human Resource Development Program for Industrial Innovation (Global)), by a grant of the Korea Health Technology R&D Project through the Korea Health Industry Development Institute (KHIDI), funded by the Ministry of Health and Welfare, Republic of Korea (grant no. HI19C1348), and by

the National Research Foundation of Korea (NRF) grant funded by the Ministry of Education, Science and Technology (2019R1A2C2085177).

ABBREVIATIONS

3D, three-dimensional; LED, light emitting diode; RC delay, Resistive-capacitive delay; 2D, two-dimensional; III-V, group III and IV; LiF, lithium fluoride; Si, silicon; Ge, germanium; BaTiO, barium titanate; HfS_2, hafnium disulfide; ZrS_2, zirconium disulfide; $CsPbBr_3$, cesium lead bromide; NaCl, sodium chloride; GaN, gallium nitride; GaAs, gallium arsenide; AlN, aluminum nitride; Al_2O_3, alumina or sapphire; III-N, group III and nitrogen/nitride; InGaP, Indium gallium phosphide; GaP, gallium phosphide; SiC, silicon carbide; Cu, copper; $SrTiO_3$, Strontium titanate; II-VI, group II and VI; I-VII, group I and VII; VO_2, vanadium oxide; i.e. that is; UV, ultraviolet

REFERENCES

(1) *International Roadmap for Devices and Systems 2022 Edition*. https://irds.ieee.org/editions/2022 (accessed 2024-02-07).
(2) Shulaker, M. M.; Wu, T. F.; Sabry, M. M.; Wei, H.; Wong, H.-S. P.; Mitra, S. Monolithic 3D Integration: A Path from Concept to Reality. In *2015 Design, Automation & Test in Europe Conference & Exhibition (DATE)*; IEEE, 2015; pp 1197–1202.
(3) Gambino, J. P.; Adderly, S. A.; Knickerbocker, J. U. An Overview of Through-Silicon-via Technology and Manufacturing Challenges. *Microelectron. Eng.* **2015**, *135*, 73–106.
(4) Kim, Y.; Cruz, S. S.; Lee, K.; Alawode, B. O.; Choi, C.; Song, Y.; Johnson, J. M.; Heidelberger, C.; Kong, W.; Choi, S.; Qiao, K.; Almansouri, I.; Fitzgerald, E. A.; Kong, J.; Kolpak, A. M.; Hwang, J.; Kim, J. Remote Epitaxy through Graphene Enables Two-Dimensional Material-Based Layer Transfer. *Nature* **2017**, *544* (7650), 340–343.
(5) Kim, H.; Liu, Y.; Lu, K.; Chang, C. S.; Sung, D.; Akl, M.; Qiao, K.; Kim, K. S.; Park, B.-I.; Zhu, M.; Suh, J. M.; Kim, J.; Baek, Y.; You, J. J.; Kang, S.; Lee, S.; Han, N. M.; Kim, C.; Choi, C.; Zhang, X.; Choi, H.-K.; Zhang, Y.; Wang, H.; Kong, L.; Afeefah, N. N.; Ansari, M. N. M.; Park, J.; Lee, K.; Yeom, G. Y.; Kim, S.; Hwang, J.; Kong, J.; Bae, S.-H.; Shi, Y.; Hong, S.; Kong, W.; Kim, J. High-Throughput Manufacturing of Epitaxial Membranes from a Single Wafer by 2D Materials-Based Layer Transfer Process. *Nat. Nanotechnol.* **2023**, *18* (5), 464–470.

(6) Kim, H.; Lu, K.; Liu, Y.; Kum, H. S.; Kim, K. S.; Qiao, K.; Bae, S.-H.; Lee, S.; Ji, Y. J.; Kim, K. H.; Paik, H.; Xie, S.; Shin, H.; Choi, C.; Lee, J. H.; Dong, C.; Robinson, J. A.; Lee, J.-H.; Ahn, J.-H.; Yeom, G. Y.; Schlom, D. G.; Kim, J. Impact of 2D–3D Heterointerface on Remote Epitaxial Interaction through Graphene. *ACS Nano* **2021**, *15* (6), 10587–10596.
(7) Yoon, H.; Truttmann, T. K.; Liu, F.; Matthews, B. E.; Choo, S.; Su, Q.; Saraswat, V.; Manzo, S.; Arnold, M. S.; Bowden, M. E.; Kawasaki, J. K.; Koester, S. J.; Spurgeon, S. R.; Chambers, S. A.; Jalan, B. Freestanding Epitaxial SrTiO3 Nanomembranes via Remote Epitaxy Using Hybrid Molecular Beam Epitaxy. *Sci. Adv.* **2022**, *8* (51), eadd5328.
(8) Manzo, S.; Strohbeen, P. J.; Lim, Z. H.; Saraswat, V.; Du, D.; Xu, S.; Pokharel, N.; Mawst, L. J.; Arnold, M. S.; Kawasaki, J. K. Pinhole-Seeded Lateral Epitaxy and Exfoliation of GaSb Films on Graphene-Terminated Surfaces. *Nat. Commun.* **2022**, *13* (1), 4014.
(9) Du, D.; Jung, T.; Manzo, S.; LaDuca, Z.; Zheng, X.; Su, K.; Saraswat, V.; McChesney, J.; Arnold, M. S.; Kawasaki, J. K. Controlling the Balance between Remote, Pinhole, and van Der Waals Epitaxy of Heusler Films on Graphene/Sapphire. *Nano Lett.* **2022**, *22* (21), 8647–8653.
(10) Kong, W.; Li, H.; Qiao, K.; Kim, Y.; Lee, K.; Nie, Y.; Lee, D.; Osadchy, T.; Molnar, R. J.; Gaskill, D. K.; Myers-Ward, R. L.; Daniels, K. M.; Zhang, Y.; Sundram, S.; Yu, Y.; hoon Bae, S.; Rajan, S.; Shao-Horn, Y.; Cho, K.; Ougazzaden, A.; Grossman, J. C.; Kim, J. Polarity Governs Atomic Interaction through Two-Dimensional Materials. *Nat. Mater.* **2018**, *17* (11), 999–1004.
(11) Kum, H. S.; Lee, H.; Kim, S.; Lindemann, S.; Kong, W.; Qiao, K.; Chen, P.; Irwin, J.; Lee, J. H.; Xie, S.; Subramanian, S.; Shim, J.; Bae, S. H.; Choi, C.; Ranno, L.; Seo, S.; Lee, S.; Bauer, J.; Li, H.; Lee, K.; Robinson, J. A.; Ross, C. A.; Schlom, D. G.; Rzchowski, M. S.; Eom, C. B.; Kim, J. Heterogeneous Integration of Single-Crystalline Complex-Oxide Membranes. *Nature* **2020**, *578* (7793), 75–81.
(12) Bae, S. H.; Lu, K.; Han, Y.; Kim, S.; Qiao, K.; Choi, C.; Nie, Y.; Kim, H.; Kum, H. S.; Chen, P.; Kong, W.; Kang, B. S.; Kim, C.; Lee, J.; Baek, Y.; Shim, J.; Park, J.; Joo, M.; Muller, D. A.; Lee, K.; Kim, J. Graphene-Assisted Spontaneous Relaxation towards Dislocation-Free Heteroepitaxy. *Nat. Nanotechnol.* **2020**, *15* (4), 272–276.
(13) Dai, L.; Zhao, J.; Li, J.; Chen, B.; Zhai, S.; Xue, Z.; Di, Z.; Feng, B.; Sun, Y.; Luo, Y.; Ma, M.; Zhang, J.; Ding, S.; Zhao, L.; Jiang, Z.; Luo, W.; Quan, Y.; Schwarzkopf, J.; Schroeder, T.; Ye, Z.-G.; Xie, Y.-H.; Ren, W.; Niu, G. Highly Heterogeneous Epitaxy of Flexoelectric BaTiO3-δ Membrane on Ge. *Nat. Commun.* **2022**, *13* (1), 2990.
(14) Wang, D.; Lu, Y.; Meng, J.; Zhang, X.; Yin, Z.; Gao, M.; Wang, Y.; Cheng, L.; You, J.; Zhang, J. Remote Heteroepitaxy of Atomic Layered Hafnium Disulfide on Sapphire through Hexagonal Boron Nitride. *Nanoscale* **2019**, *11* (19), 9310–9318.
(15) Jiang, J.; Sun, X.; Chen, X.; Wang, B.; Chen, Z.; Hu, Y.; Guo, Y.; Zhang, L.; Ma, Y.; Gao, L.; Zheng, F.; Jin, L.; Chen, M.; Ma, Z.; Zhou, Y.; Padture, N. P.; Beach, K.; Terrones, H.; Shi, Y.; Gall, D.; Lu, T.-M.; Wertz, E.; Feng, J.; Shi, J. Carrier Lifetime Enhancement in Halide Perovskite via Remote Epitaxy. *Nat. Commun.* **2019**, *10* (1), 4145.
(16) Jeong, J.; Wang, Q.; Cha, J.; Jin, D. K.; Shin, D. H.; Kwon, S.; Kang, B. K.; Jang, J. H.; Yang, W. S.; Choi, Y. S.; Yoo, J.; Kim, J. K.; Lee, S. W.; Zakhidov, A.; Hong, S.; Kim, M. J.; Hong, Y. J. Remote Heteroepitaxy of GaN Microrod Heterostructures for Deformable Light-Emitting Diodes and Wafer Recycle. *Sci. Adv.* **2020**, *6* (23), eaaz5180.

(17) Kim, H.; Kim, J. C.; Jeong, Y.; Yu, J.; Lu, K.; Lee, D.; Kim, N.; Jeong, H. Y.; Kim, J.; Kim, S. Role of Transferred Graphene on Atomic Interaction of GaAs for Remote Epitaxy. *J. Appl. Phys.* **2021**, *130* (17), 174901.
(18) Qu, Y.; Xu, Y.; Cao, B.; Wang, Y.; Wang, J.; Shi, L.; Xu, K. Long-Range Orbital Hybridization in Remote Epitaxy: The Nucleation Mechanism of GaN on Different Substrates via Single-Layer Graphene. *ACS Appl. Mater. Interfaces* **2022**, *14* (1), 2263–2274.
(19) Wang, Y.; Qu, Y.; Xu, Y.; Li, D.; Lu, Z.; Li, J.; Su, X.; Wang, G.; Shi, L.; Zeng, X.; Wang, J.; Cao, B.; Xu, K. Modulation of Remote Epitaxial Heterointerface by Graphene-Assisted Attenuative Charge Transfer. *ACS Nano* **2023**, *17* (4), 4023–4033.
(20) Liu, F.; Wang, T.; Gao, X.; Yang, H.; Zhang, Z.; Guo, Y.; Yuan, Y.; Huang, Z.; Tang, J.; Sheng, B.; Chen, Z.; Liu, K.; Shen, B.; Li, X.-Z.; Peng, H.; Wang, X. Determination of the Preferred Epitaxy for III-Nitride Semiconductors on Wet-Transferred Graphene. *Sci. Adv.* **2023**, *9* (31), eadf8484.
(21) Chen, Q.; Yang, K.; Shi, B.; Yi, X.; Wang, J.; Li, J.; Liu, Z. Principles for 2D-Material-Assisted Nitrides Epitaxial Growth. *Adv. Mater.* **2023**, *35* (18), 2211075.
(22) Li, X.; Cai, W.; An, J.; Kim, S.; Nah, J.; Yang, D.; Piner, R.; Velamakanni, A.; Jung, I.; Tutuc, E.; Banerjee, S. K.; Colombo, L.; Ruoff, R. S. Large-Area Synthesis of High-Quality and Uniform Graphene Films on Copper Foils. *Science* **2009**, *324* (5932), 1312–1314.
(23) Kong, W.; Kum, H.; Bae, S. H.; Shim, J.; Kim, H.; Kong, L.; Meng, Y.; Wang, K.; Kim, C.; Kim, J. Path towards Graphene Commercialization from Lab to Market. *Nat. Nanotechnol.* **2019**, *14* (10), 927–938.
(24) Malola, S.; Häkkinen, H.; Koskinen, P. Structural, Chemical, and Dynamical Trends in Graphene Grain Boundaries. *Phys. Rev. B* **2010**, *81* (16), 165447.
(25) Kim, J.; Park, H.; Hannon, J. B.; Bedell, S. W.; Fogel, K.; Sadana, D. K.; Dimitrakopoulos, C. Layer-Resolved Graphene Transfer via Engineered Strain Layers. *Science* **2013**, *342* (6160), 833–836.
(26) Qiao, K.; Liu, Y.; Kim, C.; Molnar, R. J.; Osadchy, T.; Li, W.; Sun, X.; Li, H.; Myers-Ward, R. L.; Lee, D.; Subramanian, S.; Kim, H.; Lu, K.; Robinson, J. A.; Kong, W.; Kim, J. Graphene Buffer Layer on SiC as a Release Layer for High-Quality Freestanding Semiconductor Membranes. *Nano Lett.* **2021**, *21* (9), 4013–4020.
(27) Journot, T.; Okuno, H.; Mollard, N.; Michon, A.; Dagher, R.; Gergaud, P.; Dijon, J.; Kolobov, A.; Hyot, B. Remote Epitaxy Using Graphene Enables Growth of Stress-Free GaN. *Nanotechnology* **2019**, *30* (50), 505603.
(28) Kim, K. S.; Kang, J. E.; Chen, P.; Kim, S.; Ji, J.; Yeom, G. Y.; Kim, J.; Kum, H. S. Atomic Layer-by-Layer Etching of Graphene Directly Grown on SrTiO3 Substrates for High-Yield Remote Epitaxy and Lift-Off. *APL Mater.* **2022**, *10* (4), 041105.
(29) Lee, S.; Abbas, M. S.; Yoo, D.; Lee, K.; Fabunmi, T. G.; Lee, E.; Kim, H. I.; Kim, I.; Jang, D.; Lee, S.; Lee, J.; Park, K.-T.; Lee, C.; Kim, M.; Lee, Y. S.; Chang, C. S.; Yi, G.-C. Pulsed-Mode Metalorganic Vapor-Phase Epitaxy of GaN on Graphene-Coated c-Sapphire for Freestanding GaN Thin Films. *Nano Lett.* **2023**, *23* (24), 11578–11585.
(30) Jeong, J.; Min, K.-A.; Shin, D. H.; Yang, W. S.; Yoo, J.; Lee, S. W.; Hong, S.; Hong, Y. J. Remote Homoepitaxy of ZnO Microrods across Graphene Layers. *Nanoscale* **2018**, *10* (48), 22970–22980.
(31) Lu, Z.; Sun, X.; Xie, W.; Littlejohn, A.; Wang, G.-C.; Zhang, S.; Washington, M. A.; Lu, T.-M. Remote Epitaxy of Copper on Sapphire through Monolayer Graphene Buffer. *Nanotechnology* **2018**, *29* (44), 445702.

(32) Kim, H.; Chang, C. S.; Lee, S.; Jiang, J.; Jeong, J.; Park, M.; Meng, Y.; Ji, J.; Kwon, Y.; Sun, X.; Kong, W.; Kum, H. S.; Bae, S.-H.; Lee, K.; Hong, Y. J.; Shi, J.; Kim, J. Remote Epitaxy. *Nat. Rev. Methods Primer* **2022**, *2* (1), 40.
(33) Shim, J.; Bae, S. H.; Kong, W.; Lee, D.; Qiao, K.; Nezich, D.; Park, Y. J.; Zhao, R.; Sundaram, S.; Li, X.; Yeon, H.; Choi, C.; Kum, H.; Yue, R.; Zhou, G.; Ou, Y.; Lee, K.; Moodera, J.; Zhao, X.; Ahn, J. H.; Hinkle, C.; Ougazzaden, A.; Kim, J. Controlled Crack Propagation for Atomic Precision Handling of Wafer-Scale Two-Dimensional Materials. *Science* **2018**, *362* (6415), 665–670.
(34) Park, J.-H.; Hu, N.; Park, M.-D.; Wang, J.; Yang, X.; Lee, D.-S.; Amano, H.; Pristovsek, M. Impact of Graphene State on the Orientation of III–Nitride. *Appl. Phys. Lett.* **2023**, *123* (12), 121601.
(35) Li, J.; Chen, M.; Samad, A.; Dong, H.; Ray, A.; Zhang, J.; Jiang, X.; Schwingenschlögl, U.; Domke, J.; Chen, C.; Han, Y.; Fritz, T.; Ruoff, R. S.; Tian, B.; Zhang, X. Wafer-Scale Single-Crystal Monolayer Graphene Grown on Sapphire Substrate. *Nat. Mater.* **2022**, *21* (7), 740–747.
(36) Toh, C. T.; Zhang, H.; Lin, J.; Mayorov, A. S.; Wang, Y. P.; Orofeo, C. M.; Ferry, D. B.; Andersen, H.; Kakenov, N.; Guo, Z.; Abidi, I. H.; Sims, H.; Suenaga, K.; Pantelides, S. T.; Özyilmaz, B. Synthesis and Properties of Free-Standing Monolayer Amorphous Carbon. *Nature* **2020**, *577* (7789), 199–203.
(37) Hong, S.; Lee, C.-S.; Lee, M.-H.; Lee, Y.; Ma, K. Y.; Kim, G.; Yoon, S. I.; Ihm, K.; Kim, K.-J.; Shin, T. J.; Kim, S. W.; Jeon, E.; Jeon, H.; Kim, J.-Y.; Lee, H.-I.; Lee, Z.; Antidormi, A.; Roche, S.; Chhowalla, M.; Shin, H.-J.; Shin, H. S. Ultralow-Dielectric-Constant Amorphous Boron Nitride. *Nature* **2020**, *582* (7813), 511–514.
(38) Joo, W.-J.; Lee, J.-H.; Jang, Y.; Kang, S.-G.; Kwon, Y.-N.; Chung, J.; Lee, S.; Kim, C.; Kim, T.-H.; Yang, C.-W.; Kim, U. J.; Choi, B. L.; Whang, D.; Hwang, S.-W. Realization of Continuous Zachariasen Carbon Monolayer. *Sci. Adv.* **2017**, *3* (2), e1601821.
(39) Han, X.; Yu, J.; Li, Z.; Wang, X.; Hao, Z.; Luo, Y.; Sun, C.; Han, Y.; Xiong, B.; Wang, J.; Li, H.; Zhang, Y.; Duan, B.; Ning, J.; Wu, H.; Wang, L. Remote Epitaxy and Exfoliation of GaN via Graphene. *ACS Appl. Electron. Mater.* **2022**, *4* (11), 5326–5332.
(40) Sangiovanni, D. G.; Gueorguiev, G.; Kakanakova-Georgieva, A. Ab Initio Molecular Dynamics of Atomic-Scale Surface Reactions: Insights into Metal Organic Chemical Vapor Deposition of AlN on Graphene. *Phys. Chem. Chem. Phys.* **2018**, *20* (26), 17751–17761.
(41) Park, J.-H.; Lee, J.-Y.; Park, M.-D.; Min, J.-H.; Lee, J.-S.; Yang, X.; Kang, S.; Kim, S.-J.; Jeong, W.-L.; Amano, H.; Dong-Seon, L. Influence of Temperature-Dependent Substrate Decomposition on Graphene for Separable GaN Growth. *Adv. Mater. Interfaces* **2019**, *6* (18), 1900821.
(42) Fan, X.; Wagner, S.; Schädlich, P.; Speck, F.; Kataria, S.; Haraldsson, T.; Seyller, T.; Lemme, M. C.; Niklaus, F. Direct Observation of Grain Boundaries in Graphene through Vapor Hydrofluoric Acid (VHF) Exposure. *Sci. Adv.* **2018**, *4* (5), eaar5170.
(43) Nemes-Incze, P.; Yoo, K. J.; Tapasztó, L.; Dobrik, G.; Lábár, J.; Horváth, Z. E.; Hwang, C.; Biró, L. P. Revealing the Grain Structure of Graphene Grown by Chemical Vapor Deposition. *Appl. Phys. Lett.* **2011**, *99* (2), 023104.
(44) Feng, T.; Zhang, S.; Yang, K.; Chen, Q.; Liang, M.; Yan, J.; Yi, X.; Wang, J.; Li, J.; Liu, Z. Graphene-Assisted Epitaxy of High-Quality GaN Films on GaN Templates. *Adv. Opt. Mater.* **2022**, *10* (24), 2201262.

(45) Park, J.-H.; Yang, X.; Lee, J.-Y.; Park, M.-D.; Bae, S.-Y.; Pristovsek, M.; Amano, H.; Lee, D.-S. The Stability of Graphene and Boron Nitride for III-Nitride Epitaxy and Post-Growth Exfoliation. *Chem. Sci.* **2021**, *12* (22), 7713–7719.
(46) Choi, J.; Jeong, J.; Zhu, X.; Kim, J.; Kang, B. K.; Wang, Q.; Park, B.-I.; Lee, S.; Kim, J.; Kim, H.; Yoo, J.; Yi, G.-C.; Lee, D.-S.; Kim, J.; Hong, S.; Kim, M. J.; Hong, Y. J. Exceptional Thermochemical Stability of Graphene on N-Polar GaN for Remote Epitaxy. *ACS Nano* **2023**, *17* (21), 21678–21689.
(47) Chang, C. S.; Kim, K. S.; Park, B.-I.; Choi, J.; Kim, H.; Jeong, J.; Barone, M.; Parker, N.; Lee, S.; Zhang, X.; Lu, K.; Suh, J. M.; Kim, J.; Lee, D.; Han, N. M.; Moon, M.; Lee, Y. S.; Kim, D.-H.; Schlom, D. G.; Hong, Y. J.; Kim, J. Remote Epitaxial Interaction through Graphene. *Sci. Adv.* **2023**, *9* (42), eadj5379.
(48) Chen, Z.; Liu, Z.; Wei, T.; Yang, S.; Dou, Z.; Wang, Y.; Ci, H.; Chang, H.; Qi, Y.; Yan, J.; Wang, J.; Zhang, Y.; Gao, P.; Li, J.; Liu, Z. Improved Epitaxy of AlN Film for Deep-Ultraviolet Light-Emitting Diodes Enabled by Graphene. *Adv. Mater.* **2019**, *31* (23), 1807345.
(49) Jang, D.; Ahn, C.; Lee, Y.; Lee, S.; Lee, H.; Kim, D.; Kim, Y.; Park, J.-Y.; Kwon, Y.-K.; Choi, J.; Kim, C. Thru-Hole Epitaxy: A Highway for Controllable and Transferable Epitaxial Growth. *Adv. Mater. Interfaces* **2023**, *10* (4), 2201406.
(50) Song, W.; Chen, Q.; Yang, K.; Liang, M.; Yi, X.; Wang, J.; Li, J.; Liu, Z. Recent Advances in Mechanically Transferable III-Nitride Based on 2D Buffer Strategy. *Adv. Funct. Mater.* **2023**, *33* (12), 2209880.
(51) Liang, D.; Wei, T.; Wang, J.; Li, J. Quasi van Der Waals Epitaxy Nitride Materials and Devices on Two Dimension Materials. *Nano Energy* **2020**, *69*, 104463.
(52) Yin, Y.; Ren, F.; Wang, Y.; Liu, Z.; Ao, J.; Liang, M.; Wei, T.; Yuan, G.; Ou, H.; Yan, J.; Yi, X.; Wang, J.; Li, J. Direct van Der Waals Epitaxy of Crack-Free AlN Thin Film on Epitaxial WS2. *Materials* **2018**, *11* (12), 2464.
(53) Ren, F.; Liu, B.; Chen, Z.; Yin, Y.; Sun, J.; Zhang, S.; Jiang, B.; Liu, B.; Liu, Z.; Wang, J.; Liang, M.; Yuan, G.; Yan, J.; Wei, T.; Yi, X.; Wang, J.; Zhang, Y.; Li, J.; Gao, P.; Liu, Z.; Liu, Z. Van Der Waals Epitaxy of Nearly Single-Crystalline Nitride Films on Amorphous Graphene-Glass Wafer. *Sci. Adv.* **2021**, *7* (31), eabf5011.
(54) Yu, Y.; Wang, T.; Chen, X.; Zhang, L.; Wang, Y.; Niu, Y.; Yu, J.; Ma, H.; Li, X.; Liu, F.; Deng, G.; Shi, Z.; Zhang, B.; Wang, X.; Zhang, Y. Demonstration of Epitaxial Growth of Strain-Relaxed GaN Films on Graphene/SiC Substrates for Long Wavelength Light-Emitting Diodes. *Light Sci. Appl.* **2021**, *10* (1), 117.
(55) Chang, H.; Liu, Z.; Yang, S.; Gao, Y.; Shan, J.; Liu, B.; Sun, J.; Chen, Z.; Yan, J.; Liu, Z.; Wang, J.; Gao, P.; Li, J.; Liu, Z.; Wei, T. Graphene-Driving Strain Engineering to Enable Strain-Free Epitaxy of AlN Film for Deep Ultraviolet Light-Emitting Diode. *Light Sci. Appl.* **2022**, *11* (1), 88.
(56) Kim, H.; Lee, S.; Shin, J.; Zhu, M.; Akl, M.; Lu, K.; Han, N. M.; Baek, Y.; Chang, C. S.; Suh, J. M.; Kim, K. S.; Park, B.-I.; Zhang, Y.; Choi, C.; Shin, H.; Yu, H.; Meng, Y.; Kim, S.-I.; Seo, S.; Lee, K.; Kum, H. S.; Lee, J.-H.; Ahn, J.-H.; Bae, S.-H.; Hwang, J.; Shi, Y.; Kim, J. Graphene Nanopattern as a Universal Epitaxy Platform for Single-Crystal Membrane Production and Defect Reduction. *Nat. Nanotechnol.* **2022**, *17* (10), 1054–1059.
(57) Guo, Y.; Sun, X.; Jiang, J.; Wang, B.; Chen, X.; Yin, X.; Qi, W.; Gao, L.; Zhang, L.; Lu, Z.; Jia, R.; Pendse, S.; Hu, Y.; Chen, Z.; Wertz, E.; Gall, D.; Feng, J.; Lu, T.-M.; Shi, J. A Reconfigurable Remotely Epitaxial VO2 Electrical Heterostructure. *Nano Lett.* **2019**, *20* (1), 33–42.

(58) Wang, P.; Pandey, A.; Gim, J.; Shin, W. J.; Reid, E. T.; Laleyan, D. A.; Sun, Y.; Zhang, D.; Liu, Z.; Zhong, Z.; Hovden, R.; Mi, Z. Graphene-Assisted Molecular Beam Epitaxy of AlN for AlGaN Deep-Ultraviolet Light-Emitting Diodes. *Appl. Phys. Lett.* **2020**, *116* (17), 171905.
(59) Huang, J.; Chen, J.; Meng, J.; Zhang, S.; Jiang, J.; Li, J.; Zeng, L.; Yin, Z.; Wu, J.; Zhang, X. Remote Heteroepitaxy of Transition Metal Dichalcogenides through Monolayer Hexagonal Boron Nitride. *Nano Res.* **2023**, 1–8.
(60) Shin, J.; Kim, H.; Sundaram, S.; Jeong, J.; Park, B.-I.; Chang, C. S.; Choi, J.; Kim, T.; Saravanapavanantham, M.; Lu, K.; Kim, S.; Kim, Y.; Kang, J.-H.; Kim, J.; Lee, D.; Lee, J.; Kim, J. S.; Lee, H. E.; Yeon, H.; Kum, H. S.; Bae, S.-H.; Bulovic, V.; Yu, K. J.; Lee, K.; Chung, K.; Hong, Y. J.; Ougazzaden, A.; Kim, J. Vertical Full-Colour Micro-LEDs via 2D Materials-Based Layer Transfer. *Nature* **2023**, *614* (7946), 81–87.
(61) Kim, Y.; Suh, J. M.; Shin, J.; Liu, Y.; Yeon, H.; Qiao, K.; Kum, H. S.; Kim, C.; Lee, H. E.; Choi, C.; Kim, H.; Lee, D.; Lee, J.; Park, B.-I.; Kang, S.; Kim, J.; Kim, S.; Perozek, J. A.; Wang, K.; Park, Y.; Kishen, K.; Kong, L.; Palacios, T.; Park, J.; Park, M.-C.; Kim, H.-J.; Lee, Y. S.; Lee, K.; Bae, S.-H.; Kong, W.; Han, J.; Kim, J. Chip-Less Wireless Electronic Skins by Remote Epitaxial Freestanding Compound Semiconductors. *Science* **2022**, *377* (6608), 859–864.
(62) Xu, R.; Huang, J.; Barnard, E. S.; Hong, S. S.; Singh, P.; Wong, E. K.; Jansen, T.; Harbola, V.; Xiao, J.; Wang, B. Y.; Crossley, S.; Lu, D.; Liu, S.; Hwang, H. Y. Strain-Induced Room-Temperature Ferroelectricity in SrTiO3 Membranes. *Nat. Commun.* **2020**, *11* (1), 3141.
(63) Huang, J.-K.; Wan, Y.; Shi, J.; Zhang, J.; Wang, Z.; Wang, W.; Yang, N.; Liu, Y.; Lin, C.-H.; Guan, X.; Hu, L.; Yang, Z.-L.; Huang, B.-C.; Chiu, Y.-P.; Yang, J.; Tung, V.; Wang, D.; Kourosh, K.-Z.; Wu, T.; Zu, X.; Qiao, L.; Li, L.-J.; Li, S. High-κ Perovskite Membranes as Insulators for Two-Dimensional Transistors. *Nature* **2022**, *605* (7909), 262–267.